Neuron, Volume *75*

Supplemental Information

Atoh1 Governs the Migration of Postmitotic Neurons that Shape Respiratory Effectiveness at Birth and Chemoresponsiveness in Adulthood

Wei-Hsiang Huang, Srinivasan Tupal, Teng-Wei Huang, Christopher S. Ward, Jeffery L. Neul, Tiemo J. Klisch, Paul A. Gray, and Huda Y. Zoghbi

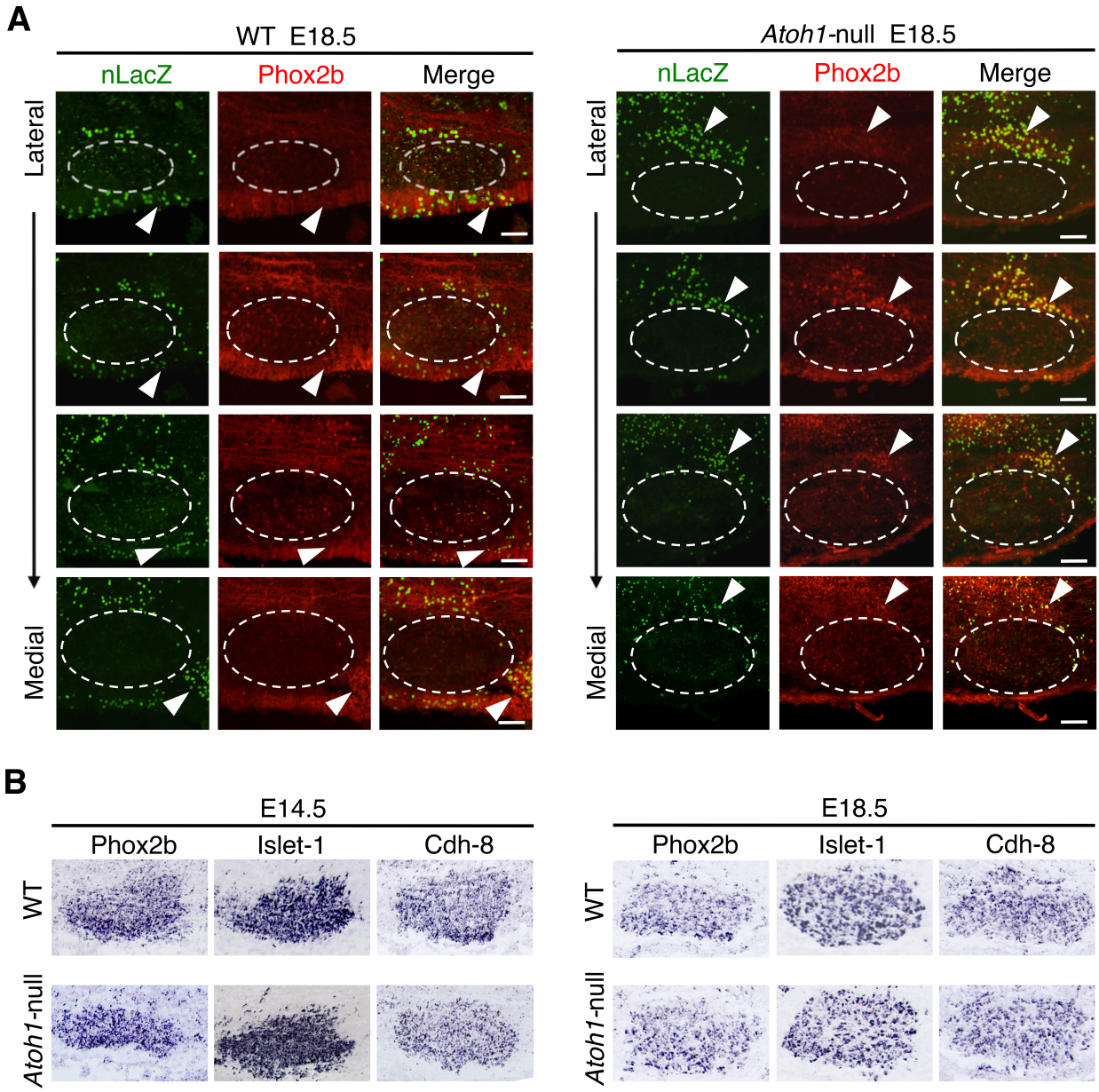

Supplemental Figure 1

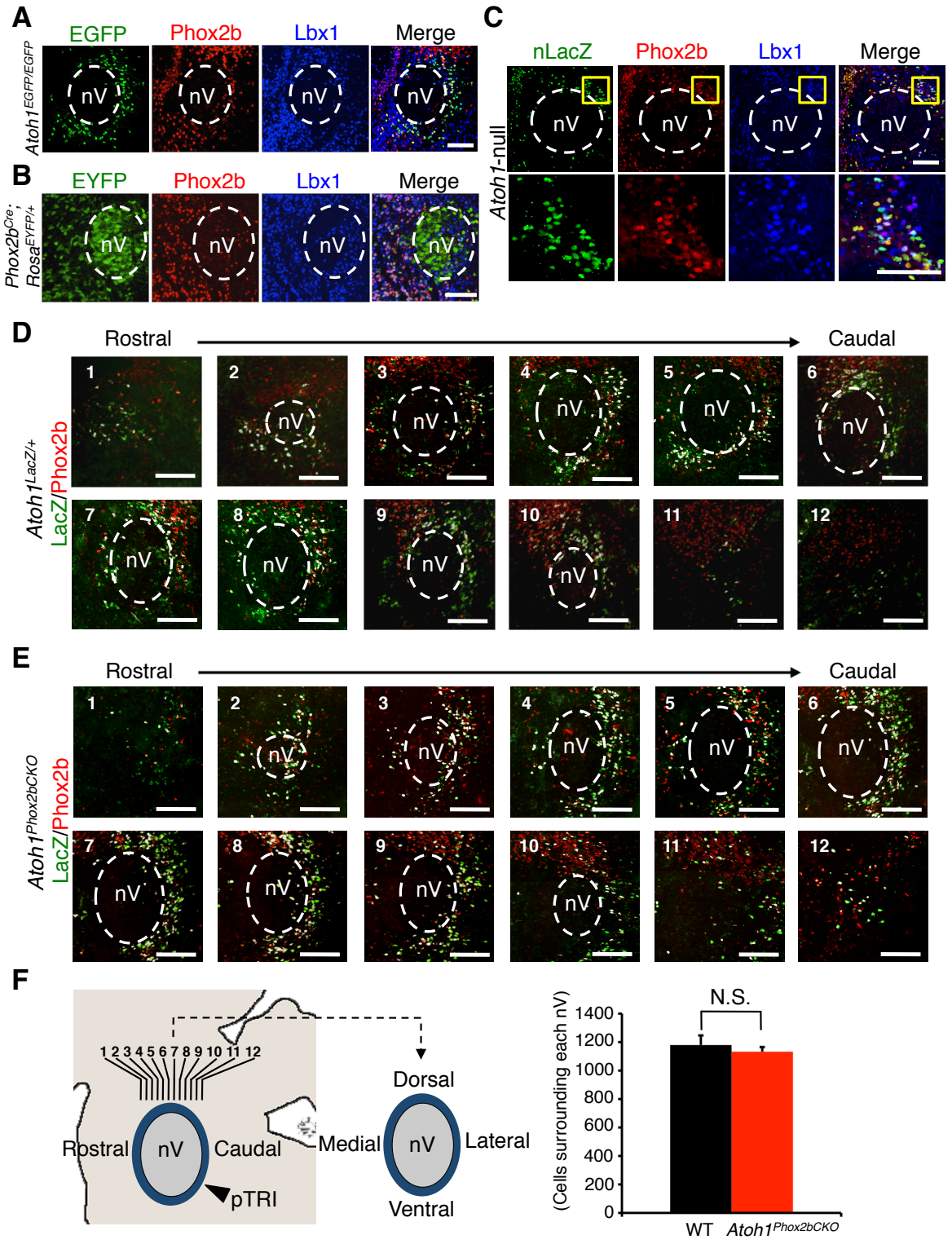

Supplemental Figure 2

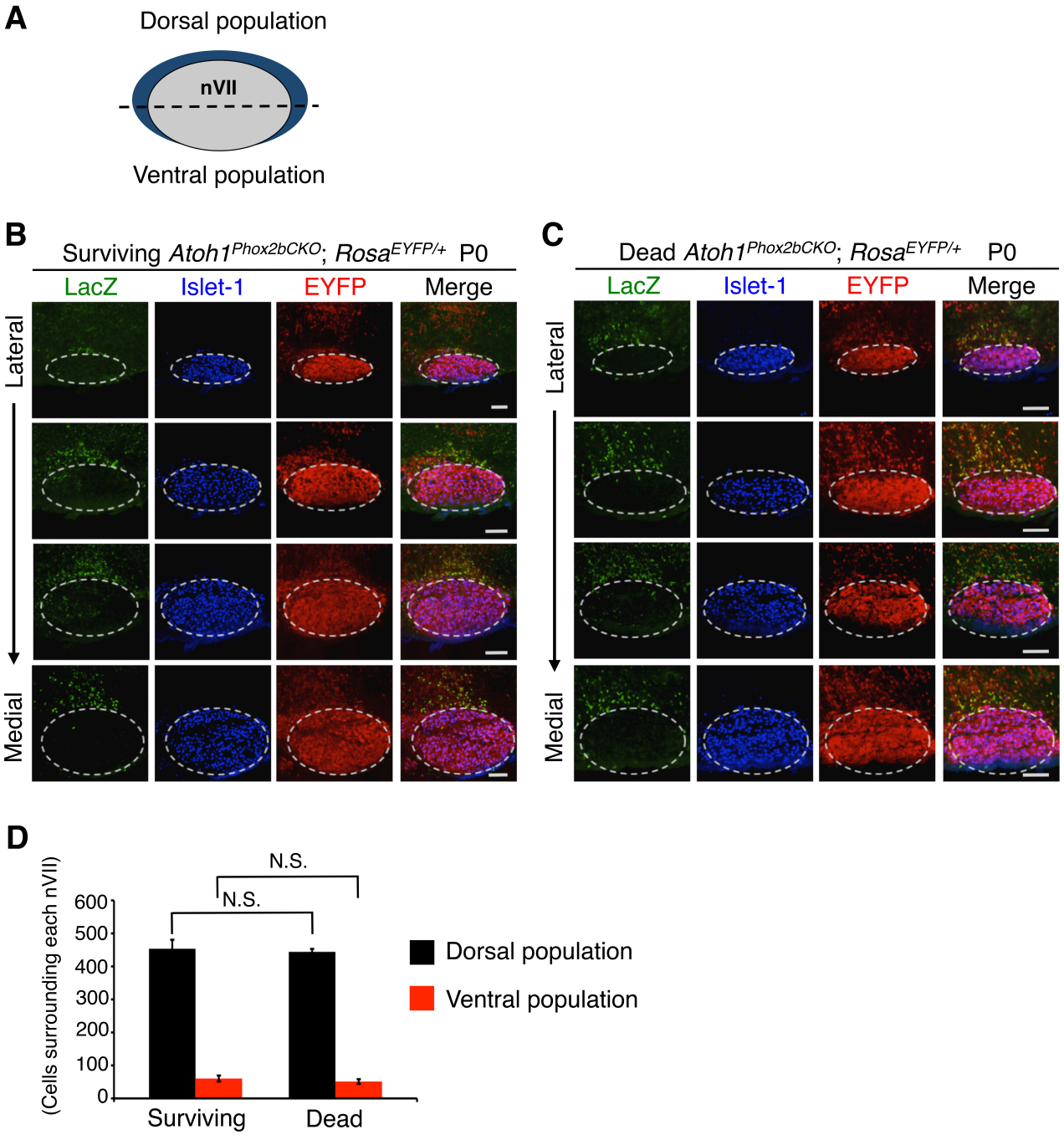

Supplemental Figure 3

SUPPLEMENTAL FIGURE LEGENDS

Supplemental Figure 1. Molecular markers of the facial motor nucleus (nVII) are unaffected in the *Atoh1*-null brainstems

(A) Representative serial sagittal sections (anterior to the left) of E18.5 WT (*Atoh1*$^{Cre/+}$; *Tau*$^{mGFP\text{-}nLacZ}$) and *Atoh1*-null (*Atoh1*$^{Cre/-}$; *Tau*$^{mGFP\text{-}nLacZ}$) brainstems. Immunofluorescence (IF) assay was performed to detect the RTN neurons (nLacZ, green, as indicated by white arrowheads) and Phox2b (red, marking both RTN and nVII (white dotted circle)). Phox2b protein expression is similar in the nVII neurons of both WT and *Atoh1*-null brainstems. (B) *In situ* hybridization of WT and *Atoh1*-null sagittal brainstem sections (anterior to the left) indicate similar mRNA expression levels of the nVII markers (*Phox2b, Islet-1* and *Cdh-8*) at E14.5 (left panel) and E18.5 (right panel), suggesting the nVII develops normally in *Atoh1*-null mice. Scale bars represent 100 μm.

Supplemental Figure 2. The paratrigeminal (pTRI) neurons remain anatomically intact in the absence of *Atoh1*

(A) Sagittal section of E16.5 *Atoh1*$^{EGFP/EGFP}$ embryo showing Atoh1-EGFP (green) is co-expressed (white) with Phox2b (red) and Lbx1 (blue) in the pTRI neurons. (B) Sagittal sections of E18.5 *Phox2b*^{Cre}; *Rosa*$^{EYFP/+}$ reporter mice showing that *Rosa-EYFP* (green) recapitulates the endogenous Phox2b expression pattern (red) and co-localizes with Lbx1 (blue) in the pTRI neurons. (C) Sagittal sections of E18.5 *Atoh1*-null (*Atoh1*$^{Cre/-}$; *Tau*$^{mGFP\text{-}nLacZ}$) embryo showing that Phox2b (red) and Lbx1 (blue) are retained in the pTRI neurons. (D-F) Quantification of pTRI neuronal number in WT (*Atoh1*$^{LacZ/+}$, D) and *Atoh1*^{Phox2bCKO} (E) brainstems.

Representative coronal sections from rostral to caudal nV showing that the pTRI neurons remain anatomically intact without *Atoh1*. Double positive cells are in white. (F) Left: Schematic with lines indicating the level of coronal section shown in (D) and (E). Right: Quantification of double positive pTRI neurons in $Atoh1^{LacZ/+}$ (D, 1179 ± 67) and $Atoh1^{Phox2bCKO}$ (E, 1132 ± 32) brainstems. The number of pTRI neurons does not significantly differ (number per brainstem, n=3 for each genotype, p=0.18, two-tailed student *t*-test). N.S.: not significantly different. Scale bars represent 100 μm.

Supplemental Figure 3. Quantification of RTN mislocalization in surviving and dead $Atoh1^{Phox2bCKO}$ newborns

(A) Schematic of nVII (gray circle) and RTN neurons (blue) in sagittal view, showing that without *Atoh1*, most of the RTN are dorsally localized. The RTN neurons are defined as dorsal/ventral population according to their position above/under the dotted line that separates the midline of nVII. (B, C) Representative serial sagittal sections (from lateral to medial) of the surviving (B) and dead (C) $Atoh1^{Phox2bCKO}$; $Rosa^{EYFP/+}$ newborn mice used for quantification in (D). Triple labeling for LacZ (marks RTN, green), Islet-1 (marks nVII, blue), and EYFP (marks $Phox2b^{Cre}$ activity, red) shows that the $Phox2b^{Cre}$ allele targets the RTN neurons in both surviving and dead $Atoh1^{Phox2bCKO}$; $Rosa^{EYFP/+}$ newborn mice. (D) Quantification of the dorsally and ventrally localized RTN neurons (defined in A) in surviving and dead $Atoh1^{Phox2bCKO}$; $Rosa^{EYFP/+}$ newborn mice at P0 (n=3 for each group). The number of RTN neurons in surviving and dead mice that localized either dorsally (453 ± 27 versus 444 ± 8, p=0.602) or ventrally (60 ± 9 versus 52 ± 7, p=0.42) is not significantly different (two-tailed student *t*-test), suggesting

similar *Phox2b*^{Cre} targeting efficiency in both situations. N.S.: not significantly different. Scale bars represent 100 μm.

Supplemental Experimental Procedures

Mouse Models

Animal housing, husbandry, and euthanasia were conducted under the guidelines of the Center for Comparative Medicine, Baylor College of Medicine. The following mouse models were used: *Atoh1*$^{Cre/+}$ (Yang et al., 2010), *Tau*$^{mGFP\text{-}nLacZ}$ (Hippenmeyer et al., 2005), *Atoh1*$^{+/-}$ (Ben-Arie et al., 1997), *Atoh1*$^{LacZ/+}$ (Ben-Arie et al., 2000), *Atoh1*$^{flox/flox}$ (Shroyer et al., 2007), *Atoh1*$^{EGFP/EGFP}$ (Rose et al., 2009), *Phox2b*^{Cre} (Rossi et al., 2011), *Rosa*$^{EYFP/EYFP}$ (Srinivas et al., 2001), and *Rosa*$^{LacZ/LacZ}$ (Soriano, 1999). PCR genotyping for the *HoxA4*^{Cre} mouse line is done using the following primers: HoxA4Cre-for 5'-GATTGCTCTTCCCCACCCTA-3' and HoxA4Cre-rev 5'-CGGACCGACGATGAAGCA-3', that amplify 507 nucleotides. For staging, noon on the day that the vaginal plug was observed counted as embryonic day 0.5 (E0.5). Yolk sac or tails were collected for PCR genotyping.

SUPPLEMENTAL REFERENCES

Ben-Arie, N., Bellen, H.J., Armstrong, D.L., McCall, A.E., Gordadze, P.R., Guo, Q., Matzuk, M.M., and Zoghbi, H.Y. (1997). Math1 is essential for genesis of cerebellar granule neurons. Nature *390*, 169-172.

Ben-Arie, N., Hassan, B.A., Bermingham, N.A., Malicki, D.M., Armstrong, D., Matzuk, M., Bellen, H.J., and Zoghbi, H.Y. (2000). Functional conservation of atonal and Math1 in the CNS and PNS. Development *127*, 1039-1048.

Hippenmeyer, S., Vrieseling, E., Sigrist, M., Portmann, T., Laengle, C., Ladle, D.R., and Arber, S. (2005). A developmental switch in the response of DRG neurons to ETS transcription factor signaling. PLoS Biol *3*, e159.

Rose, M.F., Ren, J., Ahmad, K.A., Chao, H.T., Klisch, T.J., Flora, A., Greer, J.J., and Zoghbi, H.Y. (2009). Math1 is essential for the development of hindbrain neurons critical for perinatal breathing. Neuron *64*, 341-354.

Rossi, J., Balthasar, N., Olson, D., Scott, M., Berglund, E., Lee, C.E., Choi, M.J., Lauzon, D., Lowell, B.B., and Elmquist, J.K. (2011). Melanocortin-4 receptors expressed by cholinergic neurons regulate energy balance and glucose homeostasis. Cell Metab *13*, 195-204.

Shroyer, N.F., Helmrath, M.A., Wang, V.Y., Antalffy, B., Henning, S.J., and Zoghbi, H.Y. (2007). Intestine-specific ablation of mouse atonal homolog 1 (Math1) reveals a role in cellular homeostasis. Gastroenterology *132*, 2478-2488.

Soriano, P. (1999). Generalized lacZ expression with the ROSA26 Cre reporter strain. Nat Genet *21*, 70-71.

Srinivas, S., Watanabe, T., Lin, C.S., William, C.M., Tanabe, Y., Jessell, T.M., and Costantini, F. (2001). Cre reporter strains produced by targeted insertion of EYFP and ECFP into the ROSA26 locus. BMC Dev Biol *1*, 4.

Yang, H., Xie, X., Deng, M., Chen, X., and Gan, L. (2010). Generation and characterization of Atoh1-Cre knock-in mouse line. Genesis *48*, 407-413.